



**AIAA 2000-0266**

**Subsonic and Transonic  
Dynamic Stability Characteristics  
of the X-33**

D. Tomek and R. Boyden  
NASA Langley Research Center  
Hampton, VA 23681-2199

**38th Aerospace Sciences Meeting & Exhibit**  
10-13, January 2000  
Reno, Nevada

SUBSONIC AND TRANSONIC DYNAMIC STABILITY CHARACTERISTICS OF THE X-33

Deborah M. Tomek\*† and Richmond P. Boyden\*‡

NASA Langley Research Center  
Hampton, VA

Abstract

Dynamic stability testing was conducted on a 2.5% scale model of the X-33 technology demonstrator sub-orbital flight-test vehicle. This testing was conducted at the NASA Langley Research Center (LaRC) 16-Foot Transonic Wind Tunnel with the LaRC High-Speed Dynamic Stability system. Forced oscillation data were acquired for various configurations over a Mach number range of 0.3 to 1.15 measuring pitch, roll and yaw damping, as well as the normal force due to pitch rate and the cross derivatives. The test angle of attack range was from -2 to 24 degrees, except for those cases where load constraints limited the higher angles of attack at the higher Mach numbers. A variety of model configurations with and without control surfaces were employed, including a "body alone" configuration. Stable pitch damping is exhibited for the baseline configuration throughout the angle of attack range for Mach numbers 0.3, 0.8, and 1.15. Stable pitch damping is present for Mach numbers 0.9 and 0.6 with the exception of angles 2 and 16 degrees, respectively. Constant and stable roll damping were present for the baseline configuration over the range of Mach numbers up to an angle of attack of 16 degrees. The yaw damping for the baseline is somewhat stable and constant for the angle of attack range from -2 to 8 degrees, with the exception of Mach numbers 0.6 and 0.8. Yaw damping becomes highly unstable for all Mach numbers at angles of attack greater than 8 degrees.

Nomenclature

The dynamic stability data presented are referred to the body axis system. The balance had 0.0 deg incline relative to the model  $WL = 0$ . The origin of the axes was located to correspond to the moment reference position of 66% of the body reference length or 12.514 inches. The model reference length for the pitching moment coefficients is the body reference length,  $L$ , of 18.960 inches. For the yawing and rolling moment coefficients, the reference length is the wing span,  $b$ , of 10.980 inches. The reference area,  $S$ , is 1.005 ft<sup>2</sup>. The reference values utilized for coefficient computation are shown relative to the full-scale X-33 vehicle in Table 1.

$b$	= wing span, inches
$C_l$	= rolling moment coefficient, (rolling moment/ $q_\infty S b$ )
$C_{l_p}$	= $\frac{\partial C_l}{\partial(\dot{p}b/2V)}$ , per rad
$C_{l_{\dot{p}}}$	= $\frac{\partial C_l}{\partial(\dot{p}b^2/4V^2)}$ , per rad
$C_{l_p} + C_{l_{\dot{p}}} \sin \alpha$	= damping in roll parameter, per rad
$C_{l_\beta}$	= $(\partial C_l / \partial \beta)$ , per rad
$C_{l_{\dot{\beta}}}$	= $\frac{\partial C_l}{\partial(\dot{\beta}b/2V)}$ , per rad
$C_{l_{\dot{\beta}}} \sin \alpha - k^2 C_{l_{\dot{p}}}$	= rolling moment due to roll-displacement parameter, per rad
$C_m$	= pitching-moment coefficient, (pitching moment/ $q_\infty S L$ )
$C_{m_q}$	= $\partial C_m / \partial(\dot{q}L/2V)$ , per rad
$C_{m_{\dot{q}}}$	= $\partial C_m / \partial(\dot{q}L^2/4V^2)$ , per rad
$C_{m_q} + C_{m_{\dot{q}}}$	= damping in pitch parameter, per rad
$C_{m_\alpha}$	= $(\partial C_m / \partial \alpha)$ , per rad

Copyright © 2000 by the American Institute of Aeronautics and Astronautics, Inc. No copyright is asserted in the United States under Title 17, U.S. Code. The U.S. Government has a royalty-free license to exercise all rights under the copyright claimed herein for Governmental purposes. All other rights are reserved by the copyright owner.

\*Aerospace Technologist, Research Facilities Branch, Aerodynamics, Aerothermodynamics and Acoustics Competency.

†Member AIAA

‡Senior Member AIAA

$Cm_{\dot{\alpha}}$	$= \frac{\partial Cm}{\partial(\dot{\alpha}L/2V)}$ , per rad
$Cm_{\alpha} - k^2 Cm_{\dot{\alpha}}$	= oscillatory longitudinal stability parameter, per rad
$C_n$	= yawing moment coefficient, (yawing moment/ $q_{\infty}Sb$ )
$C_{n_r}$	$= \frac{\partial C_n}{\partial(rb/2V)}$ , per rad
$C_{n_{\dot{r}}}$	$= \frac{\partial C_n}{\partial(\dot{r}b^2/4V^2)}$ , per rad
$C_{n_r} - C_{n_{\dot{r}}} \cos \alpha$	= damping in yaw parameter, per rad
$C_{n_{\beta}}$	$= (\partial C_n / \partial \beta)$ , per rad or deg
$C_{n_{\dot{\beta}}}$	$= \frac{\partial C_n}{\partial(\dot{\beta}b/2V)}$ , per rad
$C_{n_{\beta}} \cos \alpha + k^2 C_{n_{\dot{\beta}}}$	= oscillatory directional stability parameter, per rad
$k$	= reduced-frequency parameter, ( $\omega L/2V$ ) in pitch; ( $\omega b/2V$ ) in roll and yaw, rad
$L$	= body reference length, inches
$M$	= freestream Mach number
$p$	= angular velocity of model about X axis, rad/s
$q$	= angular velocity of model about Y axis, rad/s
$q_{\infty}$	= freestream dynamic pressure, psf
$r$	= angular velocity of model about Z axis, rad/s
$S$	= reference area, ft <sup>2</sup>
$V$	= freestream velocity, ft/s
$WL$	= water line
$\alpha$	= angle of attack, deg or rad
$\beta$	= angle of sideslip, deg or rad
$\omega$	= angular velocity, $2\pi f$ , rad/s

### Introduction

The X-33, a technology demonstrator sub-orbital flight-test vehicle, is being designed and tested as part of a larger program to develop a next-generation space transport vehicle. In the development of the flight control database for the X-33, Langley Research Center (LaRC) has supported Lockheed Martin in the development of the sub-orbital X-33 flight test vehicle with numerous wind tunnel tests to determine

experimentally the dynamic derivatives of the X-33 flight test vehicle. The data acquired from this series of wind tunnel tests were utilized to develop the flight control law data base for the X-33 program. This test was part of an overall program to develop a complete set of damping derivative data for the X-33 covering subsonic to supersonic Mach numbers. The focus of this paper will be to characterize the dynamic stability derivatives for the subsonic and transonic regimes.

The acquisition of the stability damping derivative data in the subsonic and transonic regimes involved modifications to the existing LaRC High-Speed Dynamic Stability System. This system was originally designed to operate in the LaRC 8-Foot Transonic Pressure Tunnel, where previous tests of this type have historically taken place. However, the 8-Foot Transonic Pressure Tunnel was closed in 1995 as part of an effort to reduce the Centers' infrastructure costs. For these X-33 tests, modifications were made to the Dynamic Stability System hardware and the software to allow a successful first time entry in the LaRC 16-Foot Transonic Tunnel (16'TT). The modifications thereby restored the capability for forced-oscillation testing at LaRC in the subsonic and transonic Mach ranges.

Forced oscillation tests of a 2.5% scale-model of the sub-orbital X-33 flight test vehicle have been conducted in the LaRC 16'TT. These tests were conducted for various configurations over a Mach number range of 0.3 to 1.15 measuring pitch, roll and yaw damping, as well as the normal force due to pitch rate and the cross derivatives: yawing moment due to roll rate and rolling moment due to yaw rate. The test angle of attack range was from -2 to 24 degrees except for those cases where load constraints limited the higher angles of attack at the higher Mach numbers. The configurations tested consisted of a baseline body arrangement with all control surfaces installed (wings and vertical tails). Breakdown component tests were then conducted with the wings removed, tails removed and both wings and tails removed for a "body alone" configuration.

### Dynamic Stability System and Apparatus

The LaRC High-Speed Dynamic Stability system utilized to conduct the test employs a technique in which the model is mechanically forced to oscillate in the tunnel air-stream at a fixed amplitude and frequency. The model is forced to oscillate in the either the pitch, yaw, or roll mode at an amplitude of about

1 degree for pitch/yaw mode and about 2.5 degrees for the roll mode. A variable speed drive motor is utilized to oscillate the test model over a variable frequency range of 3 to 30 Hz. The lower frequency limit is a result of aerodynamic loads which prevent the model from maintaining a pure sinusoidal oscillation below a frequency of 3 Hz. The great majority of these test data were taken at the frequency for velocity resonance. The most accurate measurement of the damping coefficient is obtained at the frequency of velocity resonance.<sup>2</sup> At velocity resonance, the mechanical spring in the balance, plus any aerodynamic spring contribution balances out model inertia. The only torque then required to oscillate the model at that particular frequency is the torque caused by the aerodynamic damping. The frequency range that these test data were acquired was approximately 3 to 10 Hz. The aircraft test section model is viewed as an equivalent spring-mass-damper system, with damping and spring forces provided by the interaction between the aircraft and the surrounding compressible air-stream (see Figure 1). The differential equation for this system can be expressed as:

$$I\ddot{D} + C\dot{D} + KD = Fe^{i\alpha t}$$

where  $I$  is the inertia of the rotating mass,  $K$  is the torsional spring constant,  $C$  is the damping contribution represented by the dashpot and  $Fe^{i\alpha t}$  is an applied force or moment. The mass oscillates with maximum displacement  $D$ , and at a frequency  $\omega$ . Solving for the derivatives  $\dot{D}$  and  $\ddot{D}$  where:

$$D = De^{i(\alpha t - \phi)}$$

and  $\phi$  is the phase angle between displacement and force as shown on the vector diagram in Figure 2.

By substituting we have:

$$(-I\omega^2 + iC\omega + K)D = Fe^{i\phi} = F \cos \phi + iF \sin \phi$$

The imaginary components equate to give:

$$C\omega D = F \sin \phi$$

Arriving at the stability damping coefficient for the torque component:

$$C_F = \frac{F \sin \phi}{\omega D}$$

Similarly, the real components equate to give the spring-inertia parameter:

$$K_F - I_F\omega^2 = \frac{F \cos \phi}{D}$$

Specially designed oscillating balances are utilized to mechanically force the model to oscillate. The balances operate in either pitch, yaw or roll mode. The type of balance used for both the pitch and the yaw tests, GA-16 (Figure 3a), is rolled 90 degrees with respect to the sting to change from pitch mode to yaw mode. The second type of balance, DS-05R (Figure 3b), is the roll balance. These balances, coupled with unique sting hardware, are employed to measure the input mechanical displacement and the corresponding torque required to oscillate the test model. The angular displacement is measured by means of a strain gaged mechanical spring while the force and moment load signals are measured by semi-conductor strain gage bridges bonded to the balance beams. Because of the temperature-sensitive characteristics of the semiconductor strain gage, the balances are temperature-controlled with electrical heating elements located at the front and rear of the balance beams. Balance load signals are then resolved into complex phasors relative to the displacement signal for computation of stability and damping coefficients. A recently developed dual-digital resolver system was employed that supports two complementary real-time algorithms. The algorithms include a time domain approach utilizing a numerical complex synchronous demodulation technique and a frequency domain approach utilizing Fast Fourier Transform. All data presented were acquired with the synchronous demodulation technique. The synchronous demodulation algorithm provided the needed spectral resolution required to extract just that portion of the signal at the drive frequency. Reference [1] includes a more detailed discussion of the algorithms employed with the LaRC dynamic stability system. References [2] and [3] provide a more detailed description of the LaRC forced oscillation technique and balances.

#### Model and Apparatus

All experimental data presented were obtained with a 2.5%-scale aluminum model with a steel balance adapter designed and fabricated in-house at NASA Langley. The 2.5% scale was a design limit due to tunnel blockage restrictions in the LaRC Unitary Plan Wind Tunnel where the supersonic dynamic stability data were acquired. The outer-mold-line geometry of the model was obtained from Lockheed Martin Skunk

Works and is designated as the 604B0002F/G configuration.<sup>4</sup>

The model was fabricated from 7075-T651 aluminum and included removable canted fins, body flaps, and vertical tails. The aluminum model meets a primary design goal of keeping the model inertia as low as possible so that the model resonant frequency would be above 3 Hz when using the forced-oscillation balances. Historically, operating below this resonance frequency limit can produce a non-sinusoidal motion that results in less accurate data.

The X-33 2.5%-scale model was tested in a fixed control surface baseline configuration. Data were acquired with this baseline and then with control components removed individually and globally. A sketch of the baseline X-33 full-scale model with dimensions is presented in Figure 4.

The X-33 vehicle design consists of a lifting body shape with 20-degree dihedral canted fins, two aft (windward side) body flaps, and twin vertical tails. The maximum body span between canted fin tips is 76 feet. The internal fuel tank structure drives the external body shape. The full-scale length of the X-33 vehicle is 63-feet.<sup>4</sup> The reference areas and lengths used to calculate aerodynamic and dynamic stability coefficient data for the full-scale vehicle and the 2.5% scale model are presented in Table 1. Photographs of the 2.5% X-33 model installed in the 16'TT are shown in Figure 5.

#### Test Description

The test was conducted in the NASA LaRC 16'TT which is an atmospheric, closed circuit tunnel with a Mach number range of 0.2 to 1.25. The test section of the tunnel is octagonal with a distance of 15.5 ft across the flats. Boundary layer control during transonic operation is achieved with a 35,000-hp axial flow compressor that is designed to remove up to 4.5 percent of the tunnel flow from the plenum that surrounds the test section.<sup>5</sup> A schematic of the 16'TT is presented in Figure 6.

The test results were obtained at Mach numbers 0.3, 0.6, 0.8, 0.9, 0.95, 1.05, and 1.15 over a angle of attack range from approximately 2.0 to 24.0 degrees. Table 2 summarizes nominal test conditions for this entry. The balances were kept at a constant temperature of 125 degrees Fahrenheit for the duration of data

acquisition to ensure the stability of the temperature-sensitive strain gages located on the balances.

To achieve a turbulent boundary layer over the model, No. 120 grit was applied to the upper and lower surfaces of the model. For the upper surface, a 0.1-in. wide band of grit was applied 0.9-in. aft of the fuselage nose apex and 0.4-in. aft normal to the leading edge of the canted fins or wings and the vertical tails. For the lower surface of the model, a 0.1-in. wide band was also applied 0.9-in. aft of the nose apex. Additional 0.1-in. wide bands were located 0.3-in. aft of the leading edges of the body and 0.4-in. aft of the wing normal to the leading edge.

The forced-oscillation test was conducted primarily to determine the pitch damping,  $C_{m_q} + C_{m_{\dot{\alpha}}}$ , the yaw damping,  $C_{n_r} - C_{n_{\dot{\beta}}} \cos \alpha$ , and the roll damping,  $C_{l_p} + C_{l_{\dot{\beta}}} \sin \alpha$  parameters. These parameters are all out-of-phase with the displacement of the oscillating model. The parameters in-phase with the displacement are also measured. The in-phase parameters presented in this paper are oscillatory-longitudinal stability parameter,  $C_{m_{\alpha}} - k^2 C_{m_{\dot{\alpha}}}$ , oscillatory-directional-stability parameter,  $C_{n_{\beta}} \cos \alpha + k^2 C_{n_r}$ , and rolling-moment-due-to-roll displacement parameter,  $C_{l_{\beta}} \sin \alpha - k^2 C_{l_{\dot{\beta}}}$ . A discussion of in-phase and out-of-phase parameters is provided in Reference 2.

### Experimental Results and Discussion

#### Pitching Characteristics

The oscillatory-stability parameters measured during the pitching oscillation portion of the test are presented in Figures 7a and 7b. The figures represent pitch-damping data acquired over the test Mach number range. The damping in pitch parameter for the baseline configuration is shown in Figure 7a. Negative values of the parameter represent stable damping in pitch as shown by the arrow indicators in the figures. The pitch damping is essentially constant and negative throughout the angle-of-attack range for Mach numbers of 0.3, 0.8, and 1.15, with the exception of Mach number 0.9 at an angle-of-attack of 2 degrees. The configuration becomes slightly unstable at this angle, then quickly returns to a constant, stable mode with increasing angle of attack. Stable damping in pitch was present for the Mach number 0.6 over the test angle of attack range with the exception of angle of attack of 16 degrees where the baseline configuration repeatedly exhibited positive or unstable damping. With the exception of

these angles, changing Mach number has little effect on the damping in pitch parameter for the baseline configuration.

The oscillatory-longitudinal-stability parameter for the baseline configuration is presented in Figure 7b. This is also shown over the test Mach number and angle of attack range. For the lower angles, Mach 0.3 and 0.6 remain relatively neutrally stable until an angle of attack of 8 degrees where both extend into the unstable region and grow more unstable with increasing angle of attack. For the Mach numbers 0.8 and 0.9, the stability parameter remains in the unstable region throughout the angle of attack range. The parameter also grows more unstable with increasing angle of attack. For Mach number 1.15, tunnel bearing temperature limits did not permit the acquisition of data at angles of attack greater than 8 degrees. The results of Mach 1.15 at the lower angles exhibited stable behavior with decreasing stability as the model angle of attack was increased.

Due to time limitations and program priorities, model component breakdown testing in the pitch mode was not possible during this test entry.

#### Yawing Characteristics

The oscillatory-stability parameters measured during the yawing oscillation portion of the test are presented in Figures 8 and 9. Figure 8 represents yaw damping over the test Mach number range for the baseline configuration. The damping in yaw parameter is shown in Figure 8a. Negative values of this parameter represent stable damping in yaw. The damping in yaw for the baseline configuration is relatively stable and constant over the test angle of attack range from  $-2$  to 8 degrees, with the exception of Mach numbers 0.6 and 0.8. Mach numbers 0.6 and 0.8 fluctuate around the neutral stability line through the lower angles of attack. The damping in yaw of the baseline configuration enters the unstable region for Mach numbers greater than 0.6 between 8 and 12 degrees angle of attack. For Mach number 0.6 and 0.3 the parameter fluctuates between stable and unstable as angle of attack is increased.

The oscillatory-directional-stability parameter for the baseline configuration is presented in Figure 8b. Positive values of this parameter are stable. The parameter remains relatively negative or unstable throughout the angle of attack range for all the test Mach numbers. There is a fluctuation about zero, the

neutrally stable line, at the higher alphas for the lower Mach numbers of 0.3, 0.6 and 0.8.

The yaw damping, resulting from a breakdown of model components, is shown in Figure 9a and 9b. The component breakdown results are shown for Mach number 0.9. The damping in yaw parameter is presented in Figure 9a. The yaw damping progresses into the positive or unstable region at an angle of attack of 10 degrees for the baseline configuration. As is expected, when the tails are removed from the baseline configuration the model goes unstable in yaw at a much lower angle of attack, approximately 4 degrees. For the body alone configuration, wing and tails both removed, the model is unstable at 0-degree angle of attack, is stable at 2 degrees and is unstable for angles of attack greater than 4 degrees. The X-33 vehicle can be seen to grow increasingly unstable in yaw as the test Mach number is increased and the control surfaces are eliminated.

The oscillatory-directional-stability parameter results for the component breakdown are presented in Figure 9b. Once again, positive values of this parameter are stable. For the baseline configuration, the parameter shows negative values or an unstable configuration for the test angle of attack range. Removing the tails, as is expected, has a destabilizing effect on the model with parameter values reaching further in the negative region. For the body alone configuration, wings and tails both removed, the parameter exhibits the same values as having only the tails removed. As could be expected, the wings do not contribute to the yaw damping.

#### Rolling Characteristics

The oscillatory-stability parameters measured during the rolling oscillation portion of the test are presented in Figures 10 through 13 with the damping in roll parameter given in 10(a)-13(a) and the rolling moment due to roll displacement parameter given in 10(b)-13(b). The roll damping characteristics for the baseline configuration are presented in Figure 10a. Negative values of this parameter represent stable damping in roll. The baseline configuration shows excellent stable roll damping characteristics over the range of test Mach numbers up to an angle of attack of 16 degrees. The parameter is also fairly constant over the angle of attack and Mach number range up until 16 degrees. The configuration exhibited less stable roll damping at the higher alphas, but still maintained a

negative or stable damping with the exception of Mach 0.6 at 22 degrees and 16 degrees where positive or unstable roll damping is present.

The damping in roll parameter for a component breakdown with wings removed is shown in Figures 11a, 12a and 13a for the Mach numbers 0.3, 0.9, and 1.15, respectively. Due to time limitations, the roll damping parameter was acquired for those Mach numbers only. As can be expected, with the wings removed the model remains stable and constant over the angle of attack range for both Mach numbers tested. The lifting body design of the X-33 with vertical tails and body flaps provides stable roll damping. The X-33 remains stable in roll damping even with the wings removed for all Mach numbers investigated. Also, for all the Mach numbers the roll stability remains fairly constant over the test angle of attack range.

For completeness, Figures 10b, 11b, 12b, and 13b show the results of the baseline configuration on the rolling moment due to roll-displacement parameter. This parameter was measured simultaneously with the damping in roll parameter. The first term in the parameter,  $C_{l\dot{\alpha}}\sin\alpha$ , is the aerodynamic spring term resulting from the rolling motion about the body axis at angle of attack. Because of the “ $\sin\alpha$ ” multiplier this parameter is not as useful as the effective-dihedral parameter.<sup>2,7</sup> However, the rolling moment due to roll-displacement parameter does serve to indicate gross effects such as a sign change in the dihedral effect.<sup>7</sup> As is shown in the plots, the effect on component breakdown on this parameter is minimal.

#### Data Uncertainty for the Damping Parameters

A data acquisition procedure is used with the dynamic stability system to minimize the effect of signal fluctuations due to flow separation on the model and tunnel flow unsteadiness. This procedure involves sampling a large number of filtered signal voltages for each channel at each data point and calculating the arithmetic mean and standard deviation. The arithmetic means are then used to calculate the aerodynamic parameters from the two or three data points taken at each test condition. Reference [7] provides a more detailed discussion of the dynamic stability system uncertainty.

#### Summary of Results

The LaRC High-Speed Dynamic Stability System was successful in allowing the acquisition of stability damping derivatives for the pitch, yaw, and roll modes in the subsonic and transonic regimes. The dynamic stability data acquired for the X-33 vehicle may be summarized as follows:

1. The model exhibited stable pitch damping for the baseline configuration throughout the test angle of attack range for Mach numbers 0.3, 0.8, and 1.15. Negative or stable pitch damping was present for the Mach number 0.9 over the test angle of attack range with the exception of angle of attack of 2 degrees. Stable pitch damping was present for the Mach number 0.6 over the test angle of attack range with the exception of angle of attack of 16 degrees where the baseline configuration exhibited a positive or unstable damping characteristic.
2. The yaw damping for the baseline configuration is relatively stable and constant over the test angle of attack range from -2 to 8 degrees, with the exception of Mach numbers 0.6 and 0.8. The yaw damping of the baseline configuration becomes highly unstable for all Mach numbers at angles of attack greater than 8 degrees.
3. The yaw damping enters into the positive or unstable region as the wings and tails are removed from the baseline configuration. The X-33 grows increasingly unstable in yaw as the test Mach number increases and the control surfaces are eliminated.
4. The baseline configuration showed relatively constant and stable roll damping characteristics over the range of test Mach numbers up to an angle of attack of 16 degrees. The configuration exhibited less stable roll damping at the higher alphas, but still maintained a negative value for damping with the exception of Mach 0.6 at 22 degrees and 16 degrees where unstable roll damping is present.
5. The X-33 lifting body design has stable damping in roll for the baseline configuration, and still remains stable with the wings removed for the Mach numbers investigated. As the Mach number is increased the roll stability remains fairly constant over the test angle of attack range.

Acknowledgements

The authors wish to thank the many technicians and engineers at the 16-Foot Transonic Tunnel and Dr. John S. Tripp, Dr. Ping Tcheng, Mr. Thomas L. Jordan and Mr. Floyd J. Wilcox Jr. of NASA LaRC without whose help this work would not have been possible.

References

1. Tripp, J. S.; and Tcheng, P.: Aerodynamic Stability Test Instrumentation Using Digital Signal Processing Techniques. AIAA Paper No. 94-2583, Presented at 18th Aerospace Ground Testing Conference, June 20-23, 1994, Colorado Springs, Colorado.
2. Freeman, D. C., Jr.; Boyden, R. P.; and Davenport, E. E.: Supersonic Dynamic Stability Characteristics of a Space Shuttle Orbiter. NASA TN D-8043, January 1976.
3. Braslow, A. L.; Wiley, H. G.; and Lee, C. Q.: A Rigidly Forced Oscillation System for Measuring Dynamic-Stability Parameters in Transonic and Supersonic Wind Tunnels. NASA TN D-1231, March 1962. (Supersedes NACA RM L58A28.)
4. Murphy, K.J.; Nowak, R.J.; Thompson, R.A.; Hollis, B.R.; Prabhu, R.K.: X-33 Hypersonic Aerodynamic Characteristics. AIAA-99-4162, Presented at the AIAA Atmospheric Flight Mechanics Conference and Exhibit, August 9-11, 1999, Portland, Oregon.
5. NASA LaRC 16-Foot Transonic Tunnel Facility Users Guide, NASA Langley Research Center, Wind Tunnel Enterprise.
6. Boyden, R. P.; Dress, D. A.; and Cruz, C. I.: Subsonic Dynamic Stability Characteristics of a Langley Test Techniques Demonstrator NASP Configuration. NASP TP-1016, April 1996.
7. Dress, D. A.; Boyden, R. P.; and Cruz, C. I.: Measured and Theoretical Supersonic Dynamic Stability Characteristics of a National Aero-Space Plane Configuration. Journal of Aircraft, Volume 31, Number 3, pp. 597-602, May-June 1994.

**Table 1. Reference Dimensions**

Dimension	Full Scale	2.5%-scale
<b>Sref</b>	1608 ft <sup>2</sup>	1.005 ft <sup>2</sup>
<b>Lref</b>	63.2 ft	18.960 in
<b>Bref</b>	36.6 ft	10.980 in
<b>c.g.ref (66%)</b>	41.7 ft	12.514 in

**Table 2. Nominal Test Conditions**

Mach Number	Reynolds Number	Alpha Range	Oscillation Type
0.3	2.00	A1	P,Y,R
0.6	3.45	A1	P,Y,R
0.8	3.86	A1	P,Y,R
0.9	4.00	A1	P,Y,R
0.95	3.82	A1	Y
1.05	3.89	A1	Y
1.15	4.15	A1	P,Y,R

Oscillation Type: Pitch: P, Yaw: Y, Roll: R  
 A1: - 2 to 24 deg. by 2 deg. increment

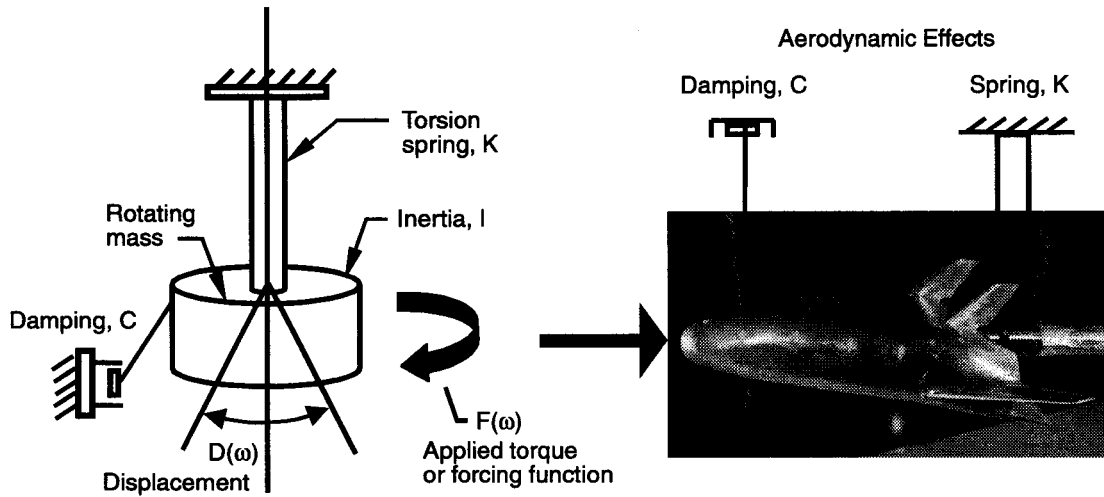


Figure 1. Dynamic Stability Spring-Mass-Damper System.

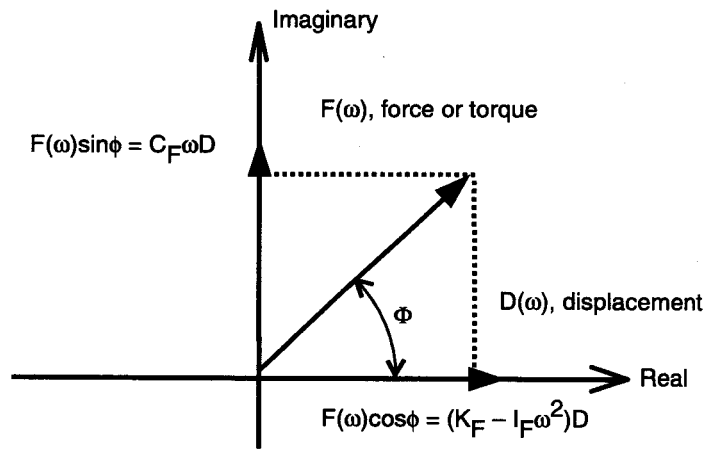
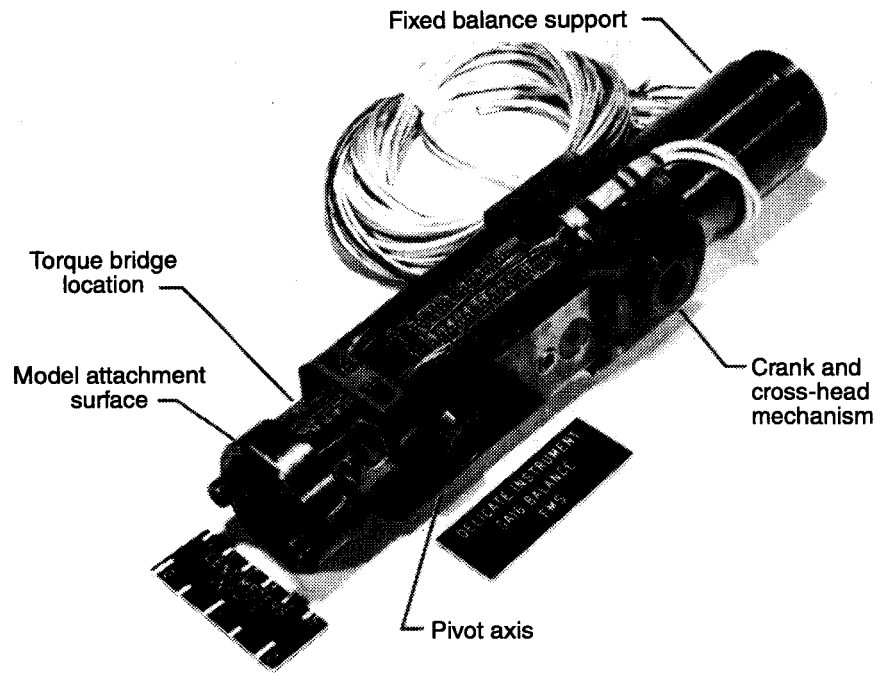
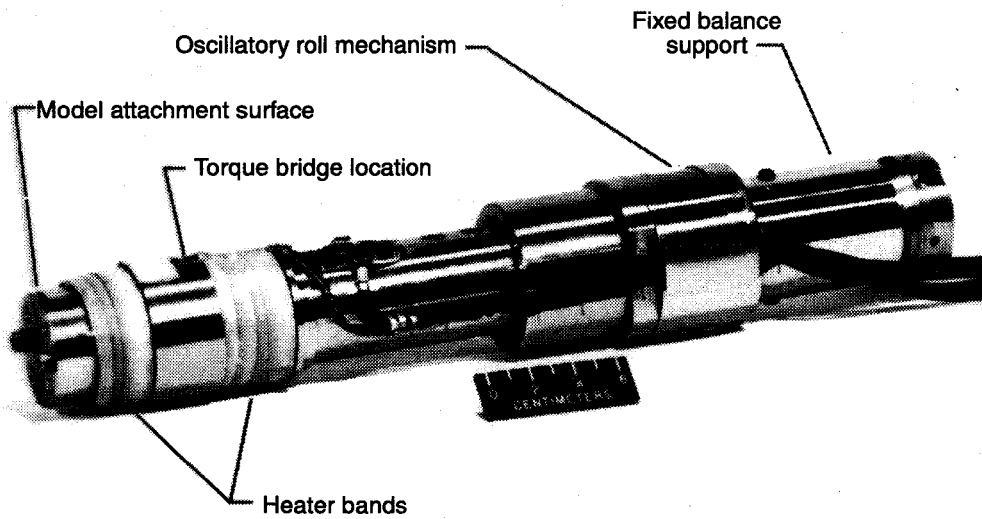


Figure 2. Phasor Diagram for the Dynamic Stability Axes.



a. GA-16 Pitch-Yaw Balance.



b. DS-05R Roll Balance.

Figure 3. LaRC Dynamic Stability System Oscillating Balances.

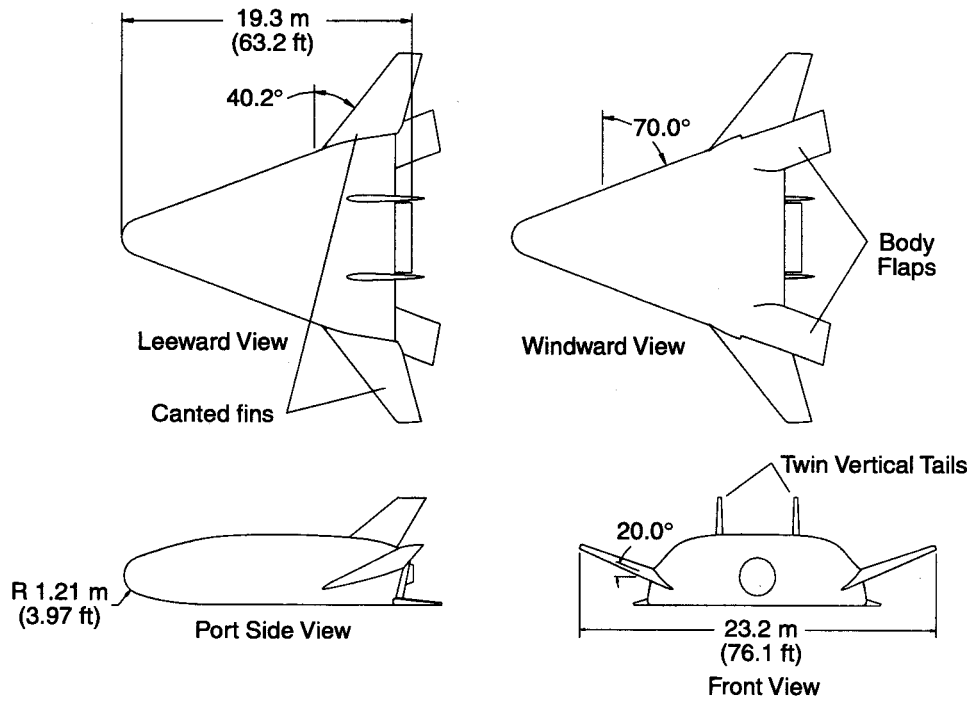


Figure 4. Sketch of Full-Scale X-33 604B0002F/G Configuration.

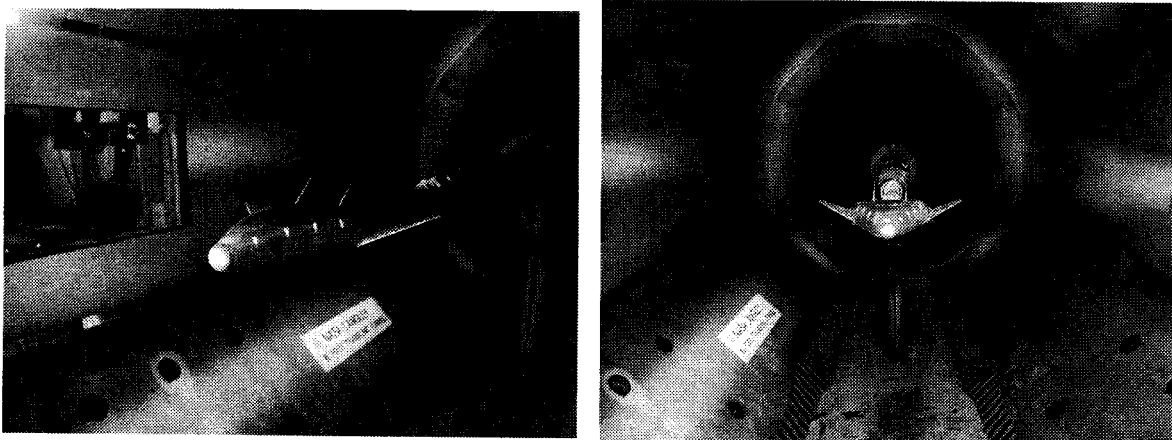


Figure 5. 2.5%-Scale X-33 Model installed in LaRC 16 FT TT.

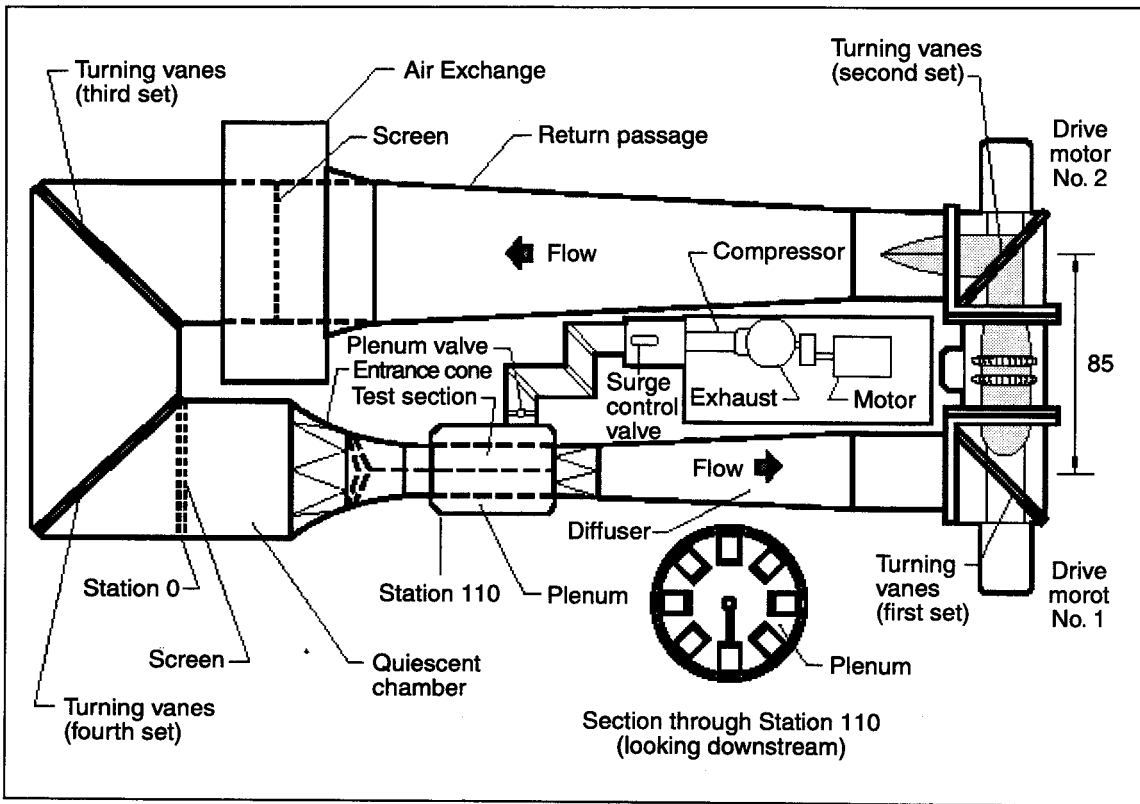


Figure 6. Schematic of the 16-Foot Transonic Tunnel. Dimensions in feet.

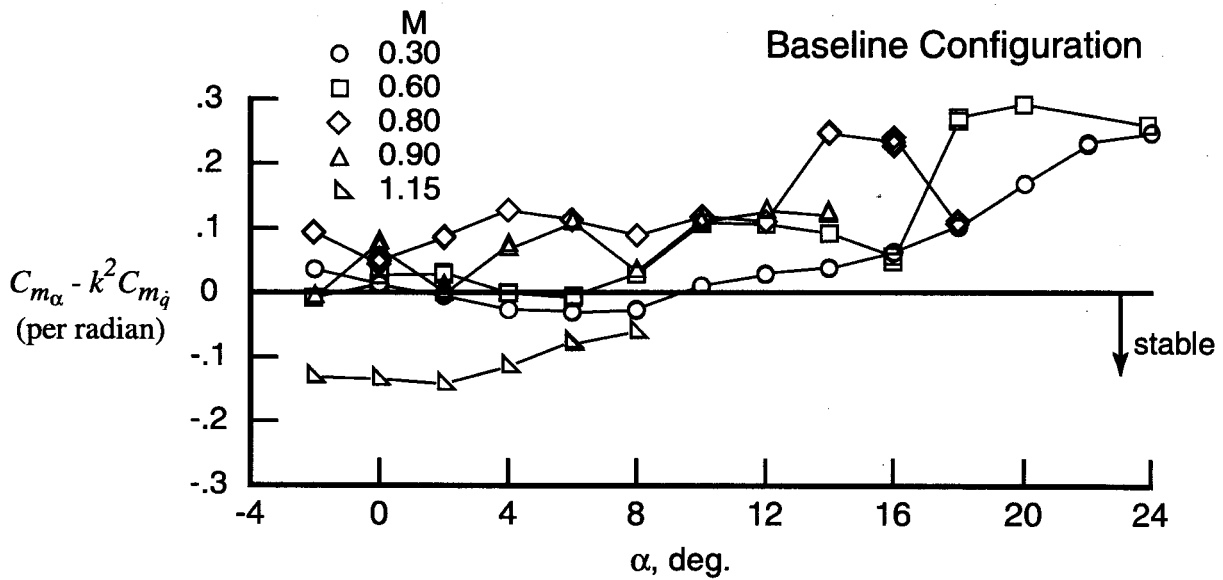
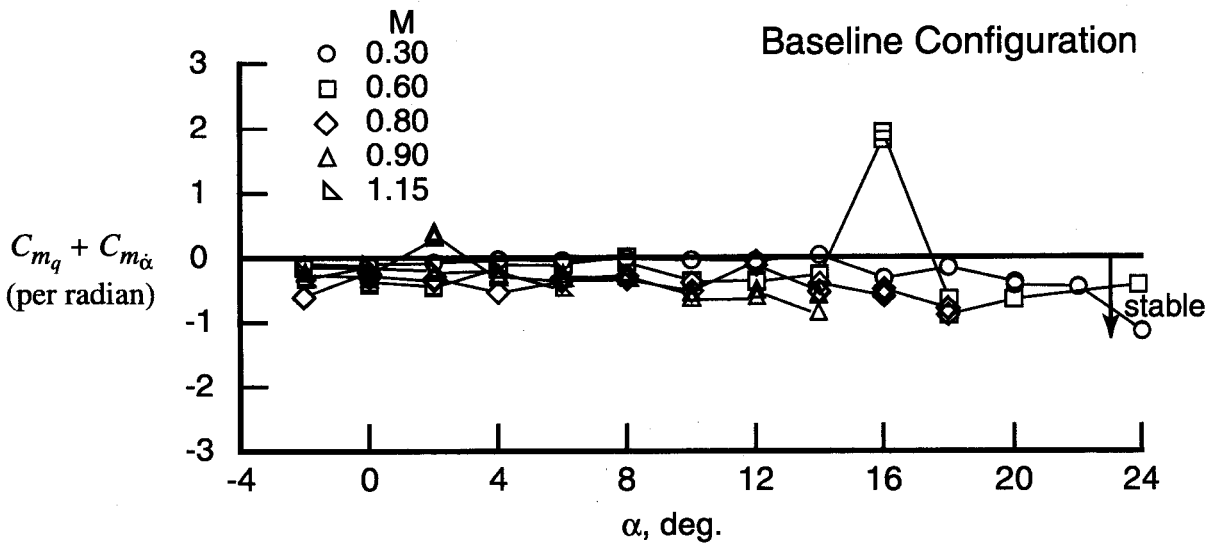


Figure 7. Results of the baseline configuration over the test Mach number range on: a) the damping-in-pitch parameter and: b) the oscillatory longitudinal-stability parameter.

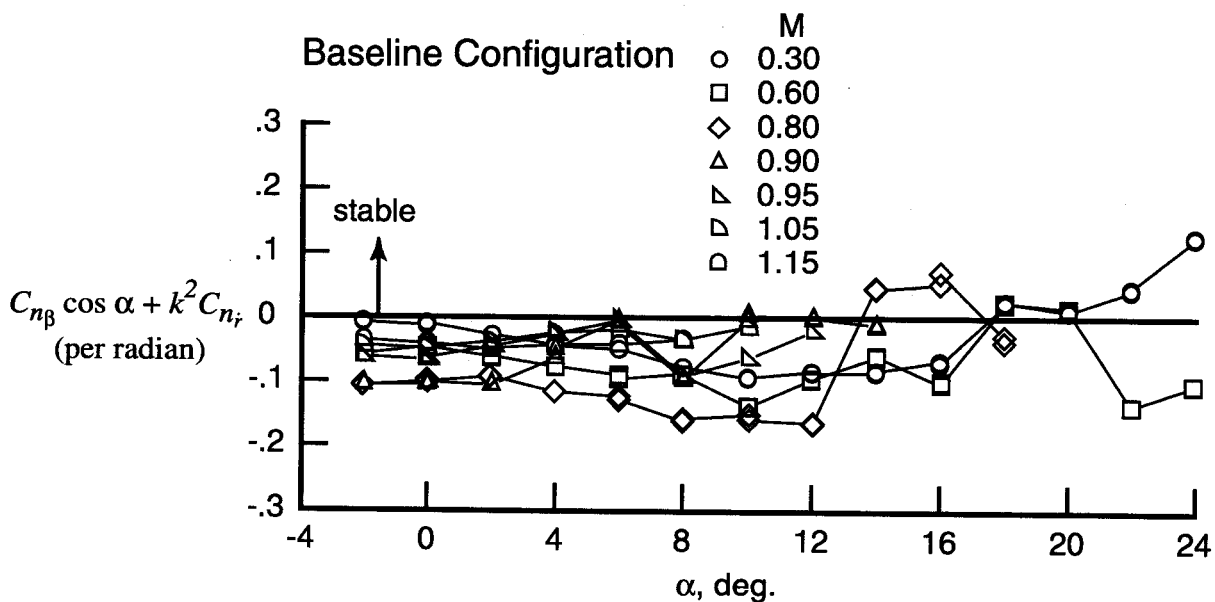
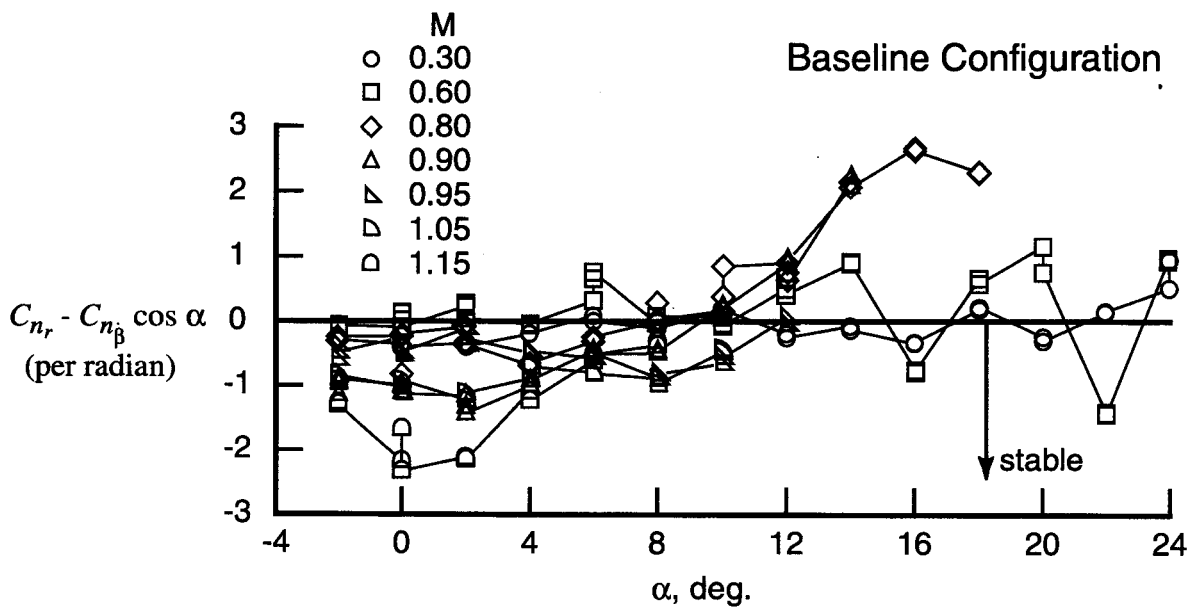


Figure 8. Results of the baseline configuration over the test Mach number range on: a) the damping-in-yaw parameter and: b) the oscillatory directional-stability parameter.

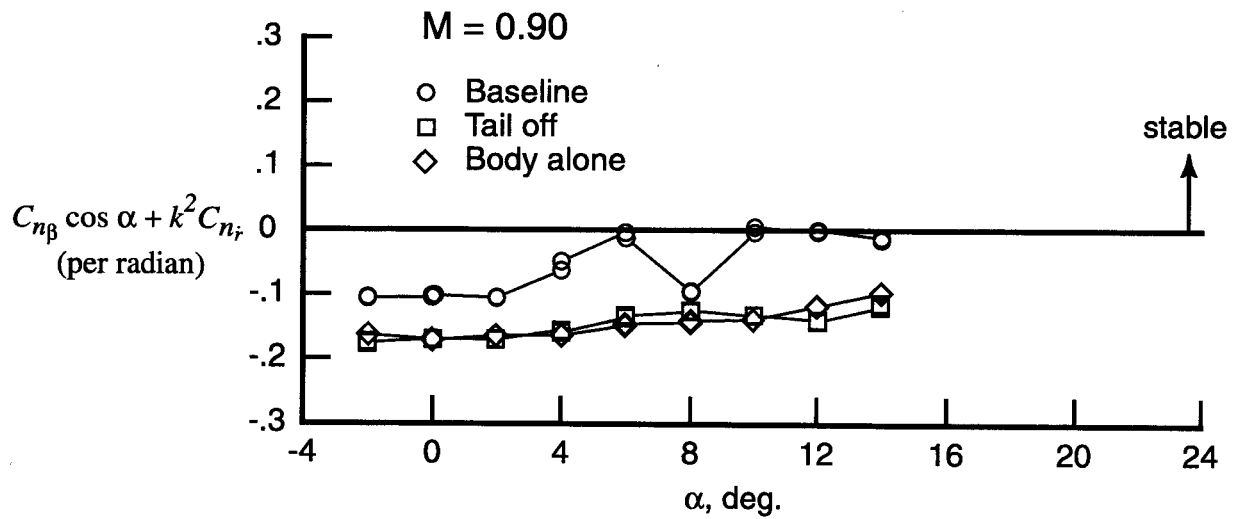
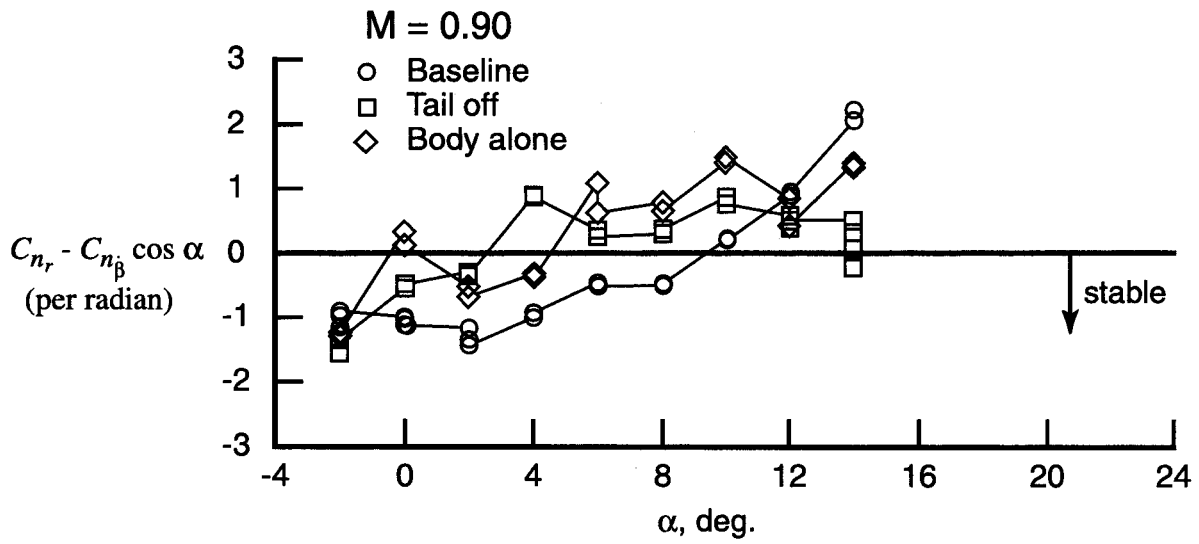


Figure 9. Results of component breakdown of the X-33 for Mach number 0.9 on: a) the damping-in-yaw parameter and: b) the oscillatory directional-stability parameter.

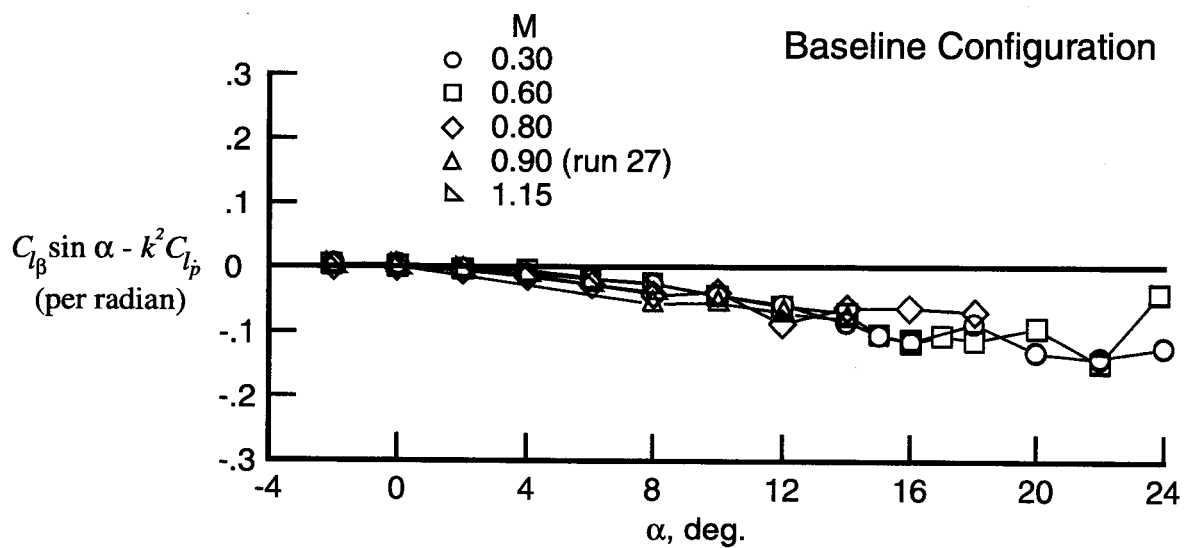
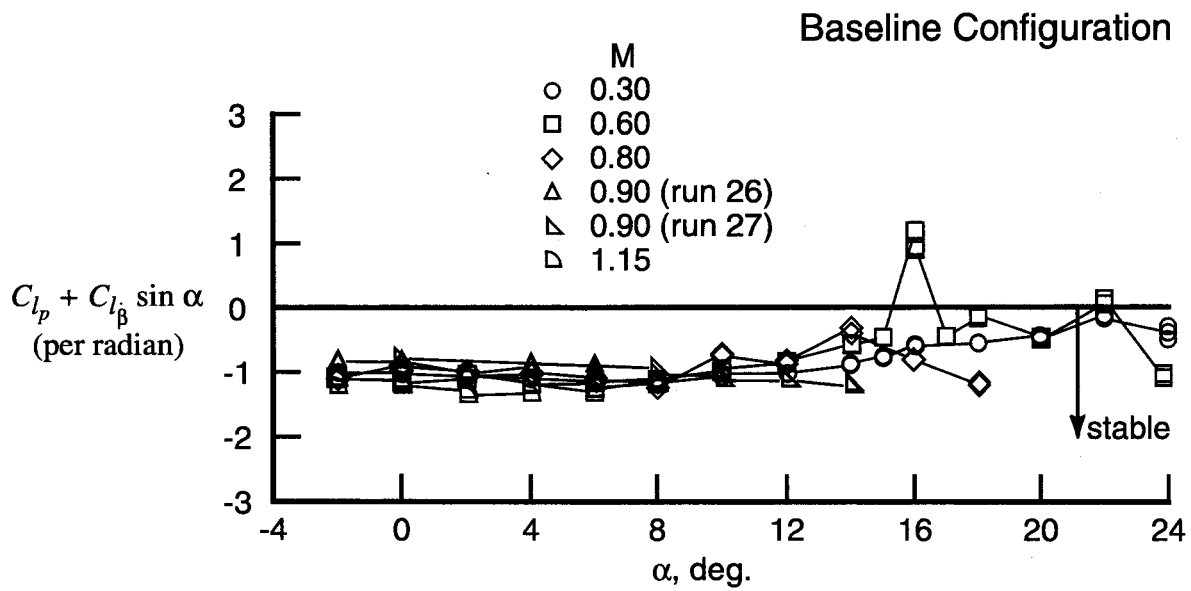


Figure 10. Results of the baseline configuration over the test Mach number range on: a) the damping-in-roll parameter and: b) the rolling moment due to roll-displacement parameter.

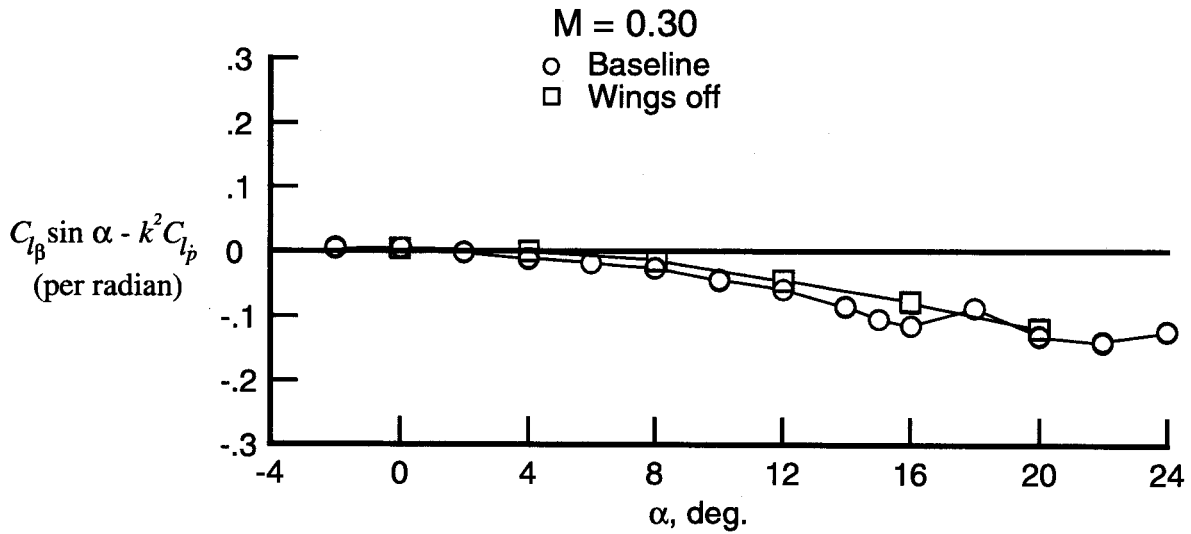
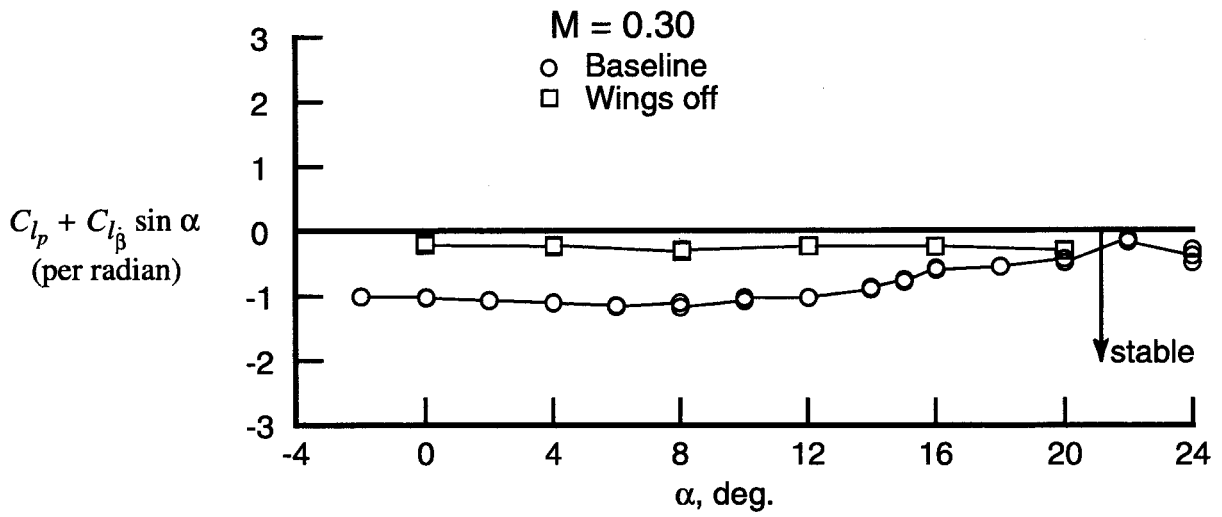


Figure 11. Results of the baseline and the wing off configuration for Mach number 0.3 on: a) the damping-in-roll parameter and: b) the rolling moment due to roll-displacement parameter.

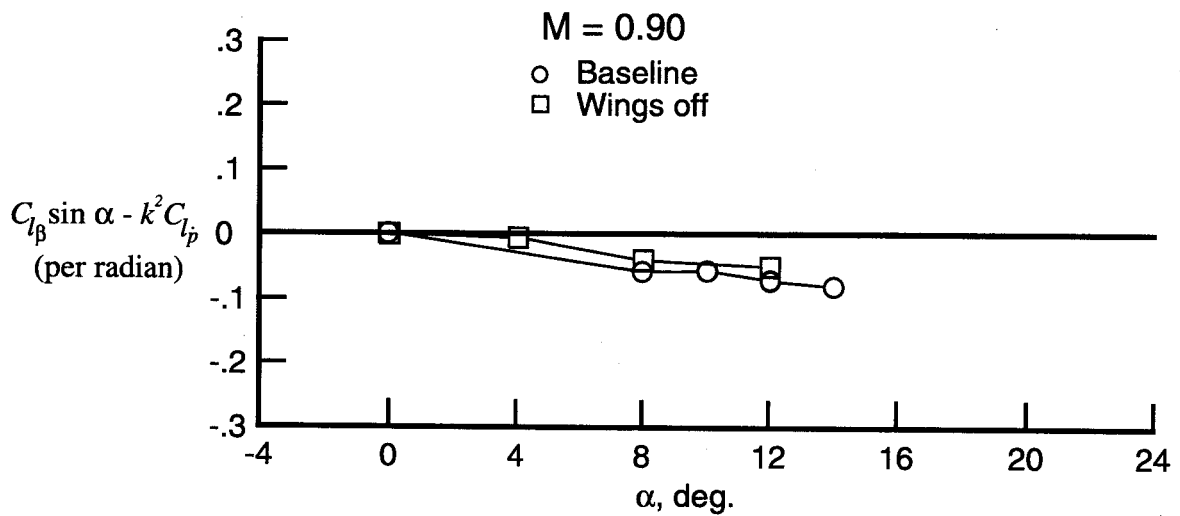
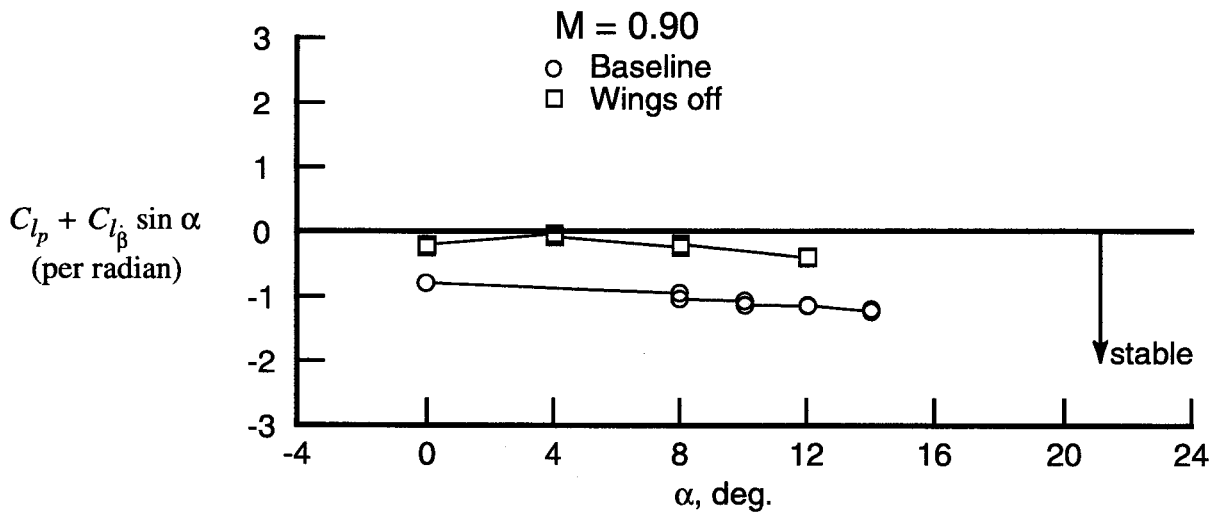


Figure 12. Results of the baseline and the wing off configuration for Mach number 0.9 on: a) the damping-in-roll parameter and: b) the rolling moment due to roll-displacement parameter.

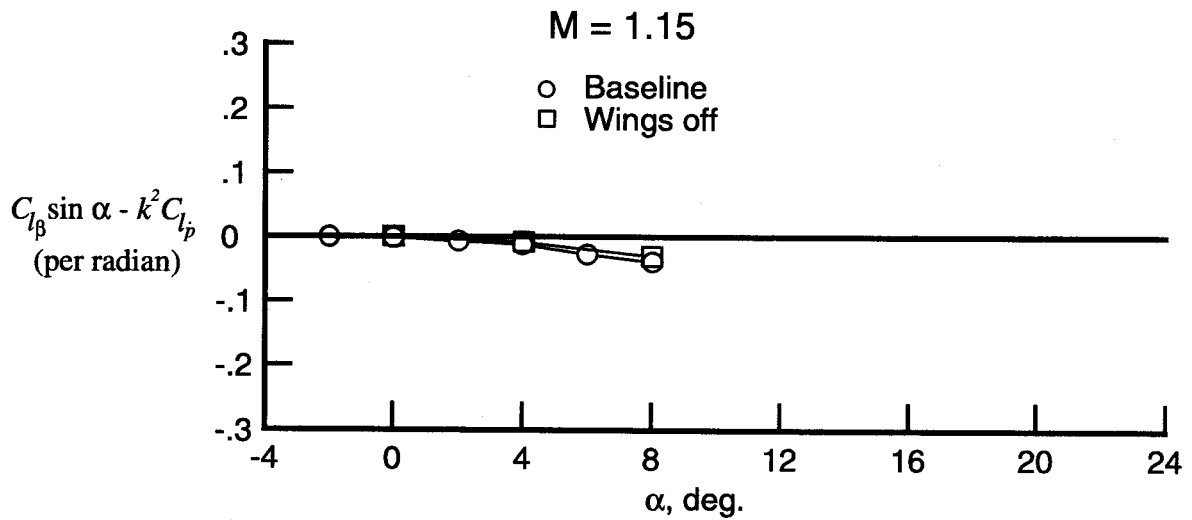
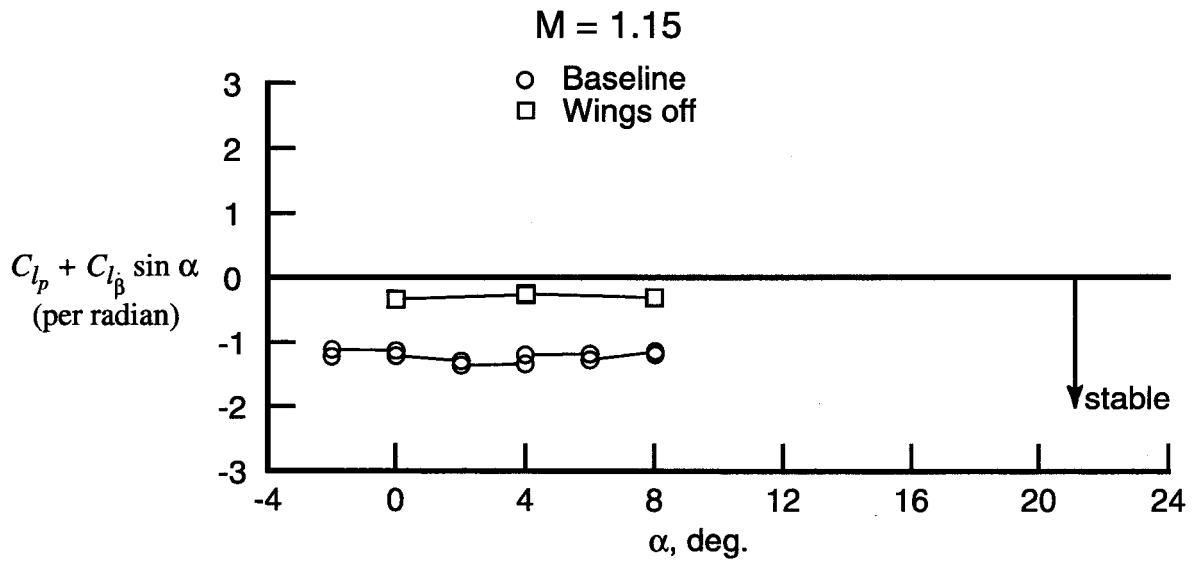


Figure 13. Results of the baseline and the wing off configuration for Mach number 1.15 on: a) the damping-in-roll-parameter and: b) the rolling moment due to roll-displacement parameter.